# Interleukin-10 Induced Activating Transcription Factor 3 Transcriptional Suppression of Matrix Metalloproteinase-2 Gene Expression in Human Prostate CPTX-1532 Cells

**Mark E. Stearns, Greg Kim, Fernando Garcia, and Min Wang**

*Department of Pathology, College of Medicine, Drexel University, Philadelphia, Pennsylvania*

## Abstract

**Aberrant expression of the 72-kDa type IV collagenase [matrix metalloproteinase (MMP)-2] is implicated in the invasion and angiogenesis process of malignant tumors. We investigated the effects of interleukin (IL)-10 on MMP-2 expression in CPTX-1532 human prostate tumor cells. Our results demonstrate that IL-10 significantly inhibited MMP-2 transcription and protein expression induced by a phorbol ester, phorbol 12-myristate 13-acetate. The inhibitory effects of IL-10 on MMP-2 expression correlated with the suppression of MMP-2 promoter activity. To determine the mechanism of IL-10 action, we examined IL-10–dependent promoter activity with luciferase constructs from a 2-kbp promoter region of the human *MMP-2* gene. We functionally characterized the promoter fragments by transient transfection experiments with CPTX-1532 cells. The experiments revealed that a cAMP responsive element binding protein (CREB) consensus domain was identified upstream of the 5′ transcriptional start site, which was highly responsive to IL-10–dependent down-regulation of promoter luciferase activity. Electrophoretic mobility shift assays combined with antibody ''supershift assays'' confirmed the data from the luciferase assays. Immunoblot assays of activating transcription factor (ATF) 3 immunoprecipitates with tyrosine specific antibodies revealed that IL-10 stimulated tyrosine phosphorylation of ATF3 to activate binding to the CREB domain and suppress MMP-2 expression. Studies with stable, IL-10 transfected CPTX-1532 subclones further showed that IL-10 failed to suppress MMP-2 expression in ATF3-deficient CPTX-1532 cells, where the ATF3 mRNA was destroyed with a DNAzyme oligonucleotide targeting the 5′ region of the mRNA. Finally, reconstitution of ATF3 successfully restored the inhibitory effects of IL-10 on MMP-2 gene expression. Taken together, these data demonstrate the critical role of tyrosine phosphorylated ATF3 and the CREB consensus domain in IL-10 suppression of MMP-2 gene expression in primary human prostate tumor cells. (Mol Cancer Res 2004; 2(7):403–16)**

## Introduction

The matrix metalloproteinases (MMPs) are a family of highly conserved zinc-dependent endopeptidases that are involved in proteolytic modeling of the extracellular matrix (1). The known substrates of MMPs include basement membrane and matrix components such as collagens, fibronectin, vitronectin, laminin, and tenascin (2, 3). The MMP selective proteolytic activity implicates MMPs in pathologic processes such as tumor invasion and angiogenesis (1, 4, 5). However, MMPs are also involved in controlling the availability of active forms of cytokines and growth factors—pro–tumor necrosis factor-α, interleukin (IL)-1β, insulin-like growth factor binding proteins, and FasL can be cleaved by MMPs (6-9). In this connection, there is a strong correlation between high levels of MMPs and diseases associated with proteolytic turnover of the extracellular matrix such as malignant tumors (1, 4). For example, abnormal expression of MMPs has been reported in cancers such as prostate, gastric, head and neck carcinomas, and melanoma (4). Two of the more exhaustively studied gelatinases, the 72-kDa type IV collagenase (MMP-2) and 97-kDa type IV collagenase (MMP-9), are directly correlated with increased malignant tumor grade and appear to play important roles in tumor invasion and metastasis (10, 11). Immunoperoxidase labeling with MMP-2 antibodies and ELISA of tissue extracts have clearly shown that malignant prostate epithelial tumor cells and associated stromal cells strongly overexpress MMP-2 (4, 5). In situ hybridization assays have further indicated that stromal cells associated with the malignant tumors may largely be responsible for the overproduction of MMP-2/MMP-9 (12). Others have shown that the selective inhibition of MMP-2 (13) and MMP-9 (14) expression can abrogate human tumor cell invasion. Likewise, expression of MMP-9 results in a metastatic phenotype in a rat sarcoma model (15), while inhibition of MMP-9 by a ribozyme suppresses the metastatic capability of the rat sarcoma cells (15) and H-*ras*– and v-*myc*–transformed rat embryo cell lines (15, 16).

Although the mechanisms regulating MMP-2 and MMP-9 gene expression are poorly understood, studies have indicated that MMP-2 activity is regulated by gene transcription, mRNA stability, proenzyme activation, and direct inhibition of enzyme activity (4, 9, 17, 18). Several studies revealed that the *MMP-2* gene can be induced by a variety of oncogene products, cytokines, mitogens, and phorbol ester (4, 13, 18) and by regulation

Received 1/24/04; revised 5/6/04; accepted 5/17/05.
The costs of publication of this article were defrayed in part by the payment of page charges. This article must therefore be hereby marked advertisement in accordance with 18 U.S.C. Section 1734 solely to indicate this fact.
**Requests for reprints:** Mark E. Stearns, Department of Pathology, College of Medicine, Drexel University, MS 435, 15th and Vine Streets, Philadelphia, PA 19085. Phone: 215-762-1597; Fax: 215-246-5918. E-mail: stearnsm1@aol.com

at the post-transcription level (mRNA stabilization). Lacraz et al. (17) compared the effects of IL-10, IL-4, IL-2, IL-6, and IFNγ on MMP-9, interstitial collagenase, and tissue inhibitor of metalloproteinase-1 (TIMP-1) synthesis in human macrophages and monocytes. They reported that IL-10 and IL-4 inhibited the production of MMP-9. Preliminary studies in our laboratory have shown that IL-10 blocks MMP-2 and MT1-MMP synthesis in primary human prostate tumor lines (13). Furthermore, IL-10 stimulation of TIMP-1 and inhibition of MMP-2/MMP-9 secretion correlated with an inhibition of angiogenesis normally induced by primary human prostate tumor cells (18). Given the potentially crucial role of MMP-2 in tumor invasion and angiogenesis, it is important to understand the molecular mechanisms by which MMP-2 expression might be inhibited in malignant cells.

In this study, we report novel observations from studies of the inhibitory effects of IL-10 on MMP-2 expression in a primary human prostate cancer tumor line termed CPTX-1532 (19). The data showed that IL-10/IL-10 receptor (IL-10R) axis signaling activation of activating transcription factor (ATF) 3 phosphorylation and ATF3 binding of the cAMP responsive element binding protein (CREB) element resulted in a significant inhibition of phorbol 12-myristate 13-acetate (PMA) induced MMP-2 expression in CPTX-1532 cells. These studies indicate the IL-10/IL-10R axis signaling pathway may play a critical role in the prevention of metalloproteinase production in prostate cancer. Moreover, the study indicates that IL-10 might be a potential therapeutic agent for the prevention of tumor invasion, angiogenesis, and metastasis.

## Results

### *Luciferase Assays With MMP-2 Promoter Constructs 1-13D*

The focus of the initial studies was to determine whether IL-10 signaling activated specific 5′ promoter elements, which suppressed PMA induced expression of the *MMP-2* gene. Initially, CPTX-1532 cells were transiently transfected with MMP-2 luciferase promoter constructs to determine the influence of PMA on the fold induction of luciferase activity. The data showed that fragments D5-D7 and wild-type (WT) exhibited the highest luciferase activity, whereas fragments D1-D3, D8, and D11 exhibited relatively intermediate activity and fragments D4 and D9-D10 + D12-D13 had relatively low activity (Fig. 1A). This suggested that multiple PMA responsive elements might be present in the MMP-2 promoter (i.e., in fragments D5-D7). In comparison, in cells treated with PMA + IL-10, the luciferase activity was reduced to near zero levels (i.e., a 22- to 30-fold reduction) in cells transfected with promoter fragments D1-D3 and by ~3-fold in cells transfected with the WT fragment. A partial reduction (i.e., by 2- to 4-fold) in luciferase activity was observed in cells transfected with fragments D4-D7 (Fig. 1B). Relatively elevated luciferase levels were recorded in cells transfected with fragments D8-D11 where the fold induction was ~2-, ~4-, ~2-, and ~4-fold, respectively (i.e., compared with that observed in PMA treated cells in Fig. 1A). Overall, the luciferase levels recorded with D12 and D13 were low independent of the treatment (compare Fig. 1A with Fig. 1B). The data suggest that IL-10 responsive factors bind a previously identified element(s) of the MMP-2 promoter (13), which includes S1 and S2 silencer elements located at the 5′ end of the intact WT fragment and D1-D3 fragments. In addition, one or more additional elements in fragments D4-D7 were responsive to IL-10, and the luciferase signal was partially reduced compared with that observed in PMA treated cells (compare Fig. 1A and Fig. 1B). In comparison, the truncated D8-D11 (particularly D8-D9) exhibited elevated luciferase levels in response to IL-10 (compare Fig. 1A and Fig. 1B), suggesting that an IL-10 sensitive suppressor element (i.e., CREB) in fragment D7 (and D1-D6, WT fragments) was removed.

To confirm that IL-10 was signaling via the IL-10R axis, the above experiments were carried out in the presence of excess IL-10R antibodies. Figure 1C showed that the inhibitory effects of IL-10 on MMP-2 promoter activity were almost completely blocked in the presence of excess IL-10R antibodies (1:200 dilution) in cells transfected with promoter fragments D1-D7 and WT. In similar experiments with the D8-D11 fragments missing the CREB element, the luciferase values were comparable with that observed in cells treated with PMA alone. Finally, similar experiments with another cytokine, IFNγ, failed to block or significantly alter PMA induction of the MMP-2 promoter activity with any of the promoter fragments, including the intact WT fragment.

The data presented were averaged from at least three independent experiments and three measurements per experiment. Statistical analysis revealed that, compared with PMA treated cells (see Fig. 1A), in Fig. 1B, the luciferase values recorded for fragments D1-D11 and WT were statistically significant ($P < 0.008$); in Fig. 1C, the values for D1-D13 and WT were not significant ($P > 0.245$); and in Fig. 1D, the $P$ values were 0.05, 0.355, 0.05, and 0.456 for D1-D3, D4-D7, D8, and D9-D13 and WT, respectively.

Figure 1E summarizes the most important data in Fig. 1A-D. Figure 1E shows the differences in luciferase activity for fragments D7 (*black*), D8 (*crosshatched*), and WT (*checkerboard*) and compares the effect of PMA, PMA + IL-10, PMA + IL-10 + IL-10R antibodies (*IL10R abs*), and IFNγ on luciferase activity. The data clearly show that IL-10 down-regulates PMA-stimulated luciferase activity in D7 and WT constructs, which contain the putative CREB suppressor element. In contrast, the luciferase activity of D8 is elevated at least 2-fold in the presence of IL-10 + PMA (compared with PMA alone), again suggesting that IL-10 suppresses the luciferase activity via the CREB element present in D7 (because it is deleted in D8). Control studies in the presence of IL-10R antibodies (in the presence of IL-10 + PMA) confirmed that the tentative CREB suppressor element in D7 fragments is indeed response to IL-10. Under these conditions, the luciferase levels are only slightly reduced from that observed in PMA treated cells. Inexplicably, the luciferase activity in D7 fragments is not elevated in the presence of IL-10 R antibodies compared with that observed in cells treated with PMA + IL-10. In summary, the data strongly suggest that IL-10 activation of the CREB suppressor element (in fragment D7) can down-regulate MMP-2 transcription in CPTX-1532 cells.

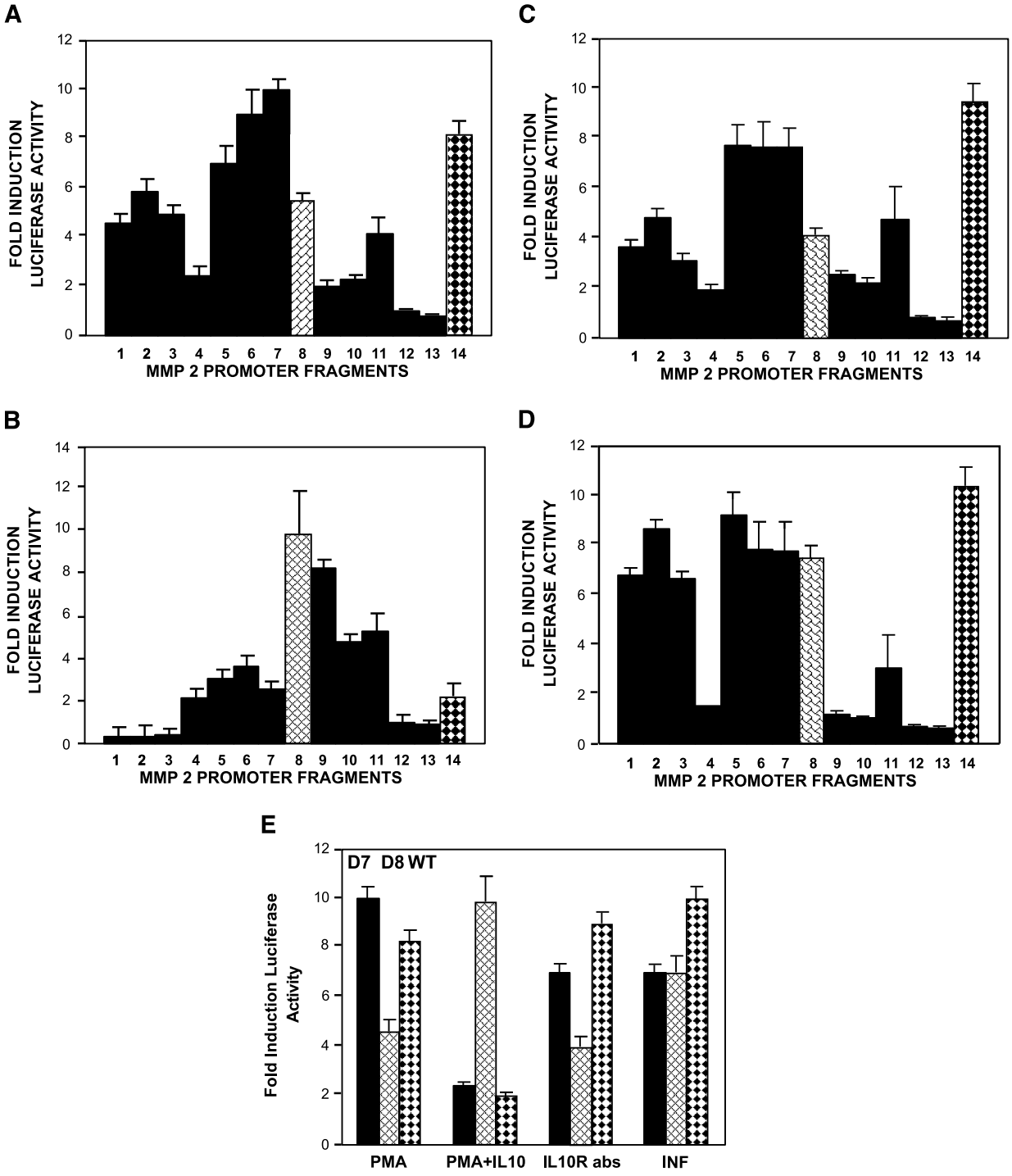


**FIGURE 1.** Luciferase assays with MMP-2 promoter constructs 1-13D and WT in transiently transfected CPTX-1532 cells. PMA induction of luciferase activity with the different MMP-2 promoter constructs, WT and fragments 1D-13D. *Column 1,* D1, which lacks the p53 site; *column 2,* D2, which lacks the first silencer element (S1); *column 3,* D3, which lacks both silencer elements (S1 and S2); *column 4,* D4, which lacks the AP-1 element; *column 5,* D5, which lacks the Ets-1 and c-Myc/c-Myb sites; *column 6,* D6, which lacks one PEA3 site and the CAAT/enhancer binding protein element; *column 7,* D7, which lacks the second PEA3 site; *column 8, crosshatched,* D8, which lacks the third PEA3 site, the CREB site, and GCN-His region; *column 9,* D9, which lacks the CREB site; *column 10,* D10, which lacks the fourth PEA3 site; *column 11,* D11, which lacks the first Sp1 element; *column 12,* D12, which lacks both Sp1 elements; *column 13,* D13, which lacks the AP-2 site; and *column 14, checkerboard,* WT, the intact MMP-2 promoter fragment. Extracts were assayed in triplicate for MMP-2 promoter luciferase activity and β-galactosidase enzyme activity as described previously (15). The luciferase activity of each sample was normalized to β-galactosidase activity to calculate relative luciferase activity before calculating the fold activation value compared with the baseline levels of luciferase vector alone. *Columns,* mean of three separate experiments (three measurements per experiment); *bars,* 1 SD. Cells plated at $1 \times 10^7$ per milliliter overnight in T175 flasks were treated for 2 hours with (**A**) 100 μmol/L PMA alone, (**B**) 100 μmol/L PMA + 15 ng/mL IL-10, (**C**) 100 μmol/L PMA + 15 ng/mL IL-10 + IL-10R antibodies, and (**D**) 100 μmol/L PMA + 10 ng/mL IFNγ. **E.** Summary of data from **A** to **D** comparing the luciferase levels observed with D7 (*black*), D8 (*crosshatched*), and WT (*checkerboard*) in cells treated with PMA, PMA + IL-10, PMA + IL-10 + IL-10R antibodies (*IL10R abs*), and IFNγ.

*Electrophoretic Mobility Shift Assays Showing IL-10 Induction of ATF3 Signaling*

Electrophoretic mobility shift assay (EMSAs) were deployed to verify whether IL-10 induced binding of one or more proteins to the CREB element. To evaluate this possibility, EMSAs were carried out with $^{32}$P-labeled CREB oligonucleotides on cytoplasmic and nuclear protein extracts following IL-10 treatment of CPTX-1532 cells for increased time intervals. EMSAs showed that a protein(s) observed to bind the CREB element was rapidly transported from the cytoplasm (Fig. 2A, *lanes 1* to *4*) to the nucleus (Fig. 2B, *lanes 1* to *4*) by ~10 to 30 minutes poststimulation with IL-10 (15 ng/mL). Moreover, the protein(s) was found exclusively in the nuclear compartment after stimulation of the cells for 60 minutes (compare Fig. 2A, *lane 4*, and Fig. 2B, *lane 4*). Following the addition of fresh medium for 4 hours, the CREB(s) was found in the cytoplasmic fraction and not in the nuclear fraction (compare Fig. 2A, *lane 5*, and Fig. 2B, *lane 5*). The protein(s) binding (*arrow*) of the $^{32}$P-labeled CREB oligonucleotide (10 ng) was blocked with 100 ng cold CREB oligonucleotide (Fig. 2C, *lane 1*) but was not blocked by lower concentrations of cold CREB oligonucleotide (Fig. 2C, *lanes 2* to *4*) or by a mutant CREB oligonucleotide at concentrations ranging from 10 to 500 ng (Fig. 2C, *lanes 5* to *9*). Note that additional studies indicated IL-10 failed to induce protein binding to PEA3 and CAAT/enhancer binding protein oligonucleotides (data not shown). The data shown were representative of results from >10 independent experiments and repeated assays of the samples prepared in these experiments.

*Antibody "Supershift" Experiments Demonstrating That ATF3 Specifically Binds the CREB Element*

To confirm that ATF3 specifically binds the CREB element, antibody "supershift" experiments were carried out. Antibody "supershift" assays (20) with increased amounts of ATF3 antibody demonstrated that the $^{32}$P-labeled CREB element binds the ATF3 protein present in nuclear extracts from IL-10 treated cells. "Supershifting" was observed at antibody concentrations >1 to 2 μg (Fig. 2D, *arrow*). Identical experiments

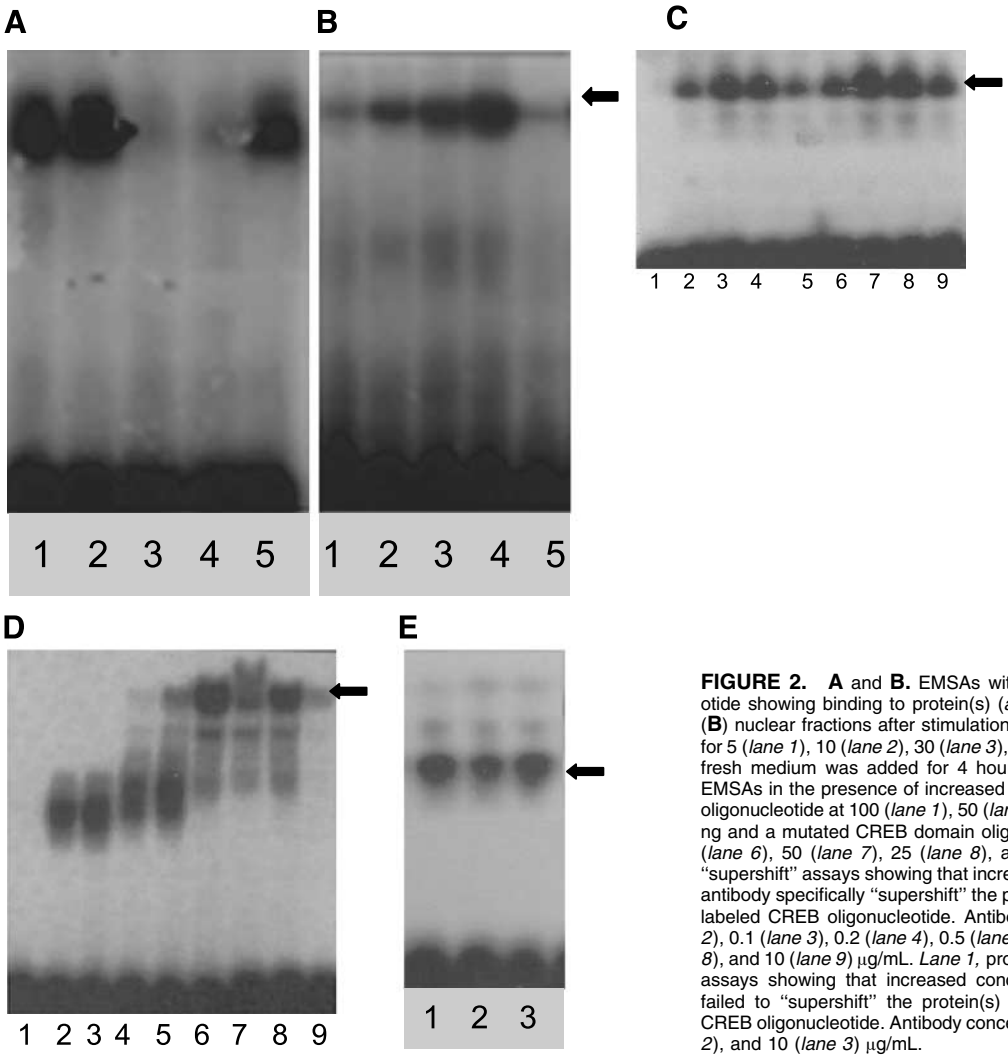


**FIGURE 2.** **A** and **B.** EMSAs with the CREB domain oligonucleotide showing binding to protein(s) (*arrow*) from (**A**) cytoplasmic and (**B**) nuclear fractions after stimulation of the cells with 15 ng/mL IL-10 for 5 (*lane 1*), 10 (*lane 2*), 30 (*lane 3*), and 60 (*lane 4*) minutes. *Lane 5,* fresh medium was added for 4 hours. **C.** Cold competition assays. EMSAs in the presence of increased amounts of the unlabeled CREB oligonucleotide at 100 (*lane 1*), 50 (*lane 2*), 25 (*lane 3*), and 10 (*lane 4*) ng and a mutated CREB domain oligonucleotide at 500 (*lane 5*), 100 (*lane 6*), 50 (*lane 7*), 25 (*lane 8*), and 10 (*lane 9*) ng. **D.** Antibody "supershift" assays showing that increased concentrations of the ATF3 antibody specifically "supershift" the protein(s) (*arrow*) binding the $^{32}$P-labeled CREB oligonucleotide. Antibody concentrations were 0 (*lane 2*), 0.1 (*lane 3*), 0.2 (*lane 4*), 0.5 (*lane 5*), 1 (*lane 6*), 2 (*lane 7*), 5 (*lane 8*), and 10 (*lane 9*) μg/mL. *Lane 1,* probe only. **E.** Antibody "supershift" assays showing that increased concentrations of the Sp1 antibody failed to "supershift" the protein(s) (*arrow*) binding the $^{32}$P-labeled CREB oligonucleotide. Antibody concentrations were 2 (*lane 1*), 5 (*lane 2*), and 10 (*lane 3*) μg/mL.

with a Sp1 antibody at increased concentrations failed to induce "supershifting" of the DNA-protein complex (Fig. 2E, *lanes 1* to *3*). The results were representative of four independent experiments.

### *Antibody Immunoprecipitation Assays Showing IL-10 Induction of ATF3 Phosphorylation/Signaling*

To learn more about the mechanism of action of IL-10, immunoprecipitation assays were carried out to determine whether IL-10 triggered tyrosine phosphorylation of ATF3. Western blots of immunoprecipitates obtained with ATF3 antibodies indicated that the 22-kDa ATF3 protein was uniformly expressed in CPTX-1532 cells treated with either PMA + IL-10, PMA, or IL-10 (Fig. 3A, *lanes 1* to *3*), respectively). More importantly, the corresponding immunoblots of the same samples with ATF3 antiphosphorylated tyrosine antibodies revealed that ATF3 was not tyrosine phosphorylated in extracts from cells treated with PMA + IL-10 (Fig. 3A, *lane 4*) or IL-10 alone (Fig. 3A, *lane 6*) but was tyrosine phosphorylated in extracts of cells exposed to PMA alone (Fig. 3A, *lane 5*). Following immunoprecipitation of ATF3 antigen with ATF3 antibodies, Western blots with ATF3 antiphosphotyrosine antibodies further showed that pretreatment of the cells with IL-10 alone (Fig. 3B, *lane 1*) and IL-10 + PMA (Fig. 3B, *lane 3*) blocked the tyrosine phosphorylation of the ATF3 protein. In cells treated with PMA alone (Fig. 3B, *lane 2*) or PMA + IL-10 + IL-10R antibodies (Fig. 3B, *lane 4*), phosphorylated ATF3 protein was detected in the nuclear protein extracts. Note that Western blots (Fig. 3C, *lanes 1* to *4*) showed that the crude protein extracts used in Fig. 3B, *lanes 1* to *4*), respectively, contained similar amounts of the 22-kDa ATF3 (*arrow*) and β-actin, indicating that gel loading artifacts did not account for the data. Densitometry measurements (A 600 nm) comparing the ratios of ATF3/β-actin (in five experiments) showed that the ratios were 0.2 ± 0.07, 0.23 ± 0.06, 0.26 ± 0.07, and 0.27 ± 0.08 (with $P > 0.456$ compared with untreated cells), indicating that no significant change in the expression levels of ATF3 arose in response to IL-10, PMA, IL-10 + PMA, and IL-10 + PMA + IL-10R antibodies. Taken together, these data from at least seven independent experiments indicate that PMA triggered tyrosine phosphorylation and signaling by ATF3 protein and that IL-10 blocked this process.

### *Influence of ATF3 DNAzyme-1Pas on ATF3 mRNA Expression in CPTX-1532 Cells*

To evaluate the role of ATF3 in the regulation of MMP-2 expression, a "ribozyme-like" ATF3 DNAzyme-1Pas (antisense) oligonucleotide (31-mer; which specifically cleaves ATF3 mRNA) was employed to "knock out" ATF3 expression. Initially, the uptake of ATF3 DNAzyme-1P was examined in CPTX-1532 cells. The cells were incubated with 5 μmol/L FAM-labeled ATF3 DNZ ZYM-1Pas or unlabeled ATF3 DNAzyme-1Pas for various periods of time or at increased concentrations for 12 hours. A time-dependent increase in oligonucleotide uptake of ~120 mean fluorescent reading units occurred over 2 to 9 hours, and incubation for longer intervals failed to increase uptake substantially. Likewise, the

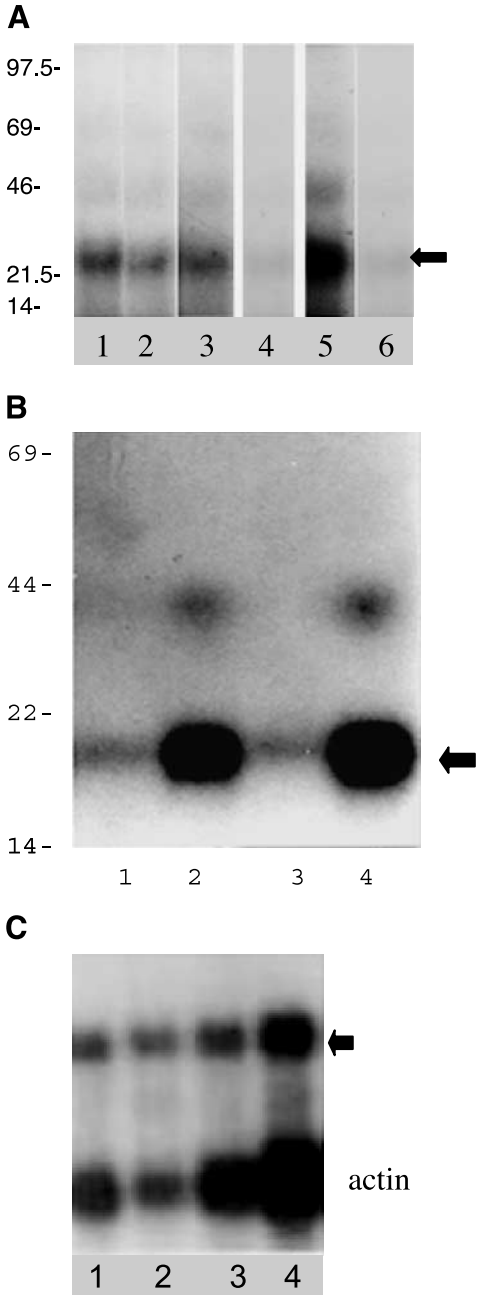


**FIGURE 3.** **A.** Immunoprecipitates with ATF3 antibodies of ~22-kDa ATF3 protein (*arrow*). Western blots of the samples were with either ATF3 antibodies (1:100 dilution; *lanes 1* to *3*) or tyrosine phosphorylated ATF3 antibodies (1:20 dilution; *lanes 4* to *6*). Crude protein extracts were from CPTX-1532 cells treated for 2 hours with 100 μmol/L PMA + 15 ng/mL IL-10 (*lanes 1* and *4*), 100 μmol/L PMA alone (*lanes 2* and *5*), and 15 ng/mL IL-10 alone (*lanes 3* and *6*). **B.** Immunoprecipitates with ATF3 antibodies were blotted with tyrosine phosphorylated ATF3 abs (1:200 dilution). Nuclear protein extracts were from CPTX-1532 cells pretreated with 15 ng/mL IL-10 (*lane 1*), 100 μmol/L PMA (*lane 2*), 15 ng/mL IL-10 + 100 μmol/L PMA (*lane 3*), and 100 μmol/L PMA + 15 ng/mL IL-10 + IL-10R antibodies (*lane 4*). **C.** Immunoblots with AFT3 (*arrow*) and β-actin antibodies (*lower band*) of the crude protein extracts used in the immunoprecipitation assays in **B** (*lanes 1* to *4*).

concentration-dependent uptake of ATF3 DNAzyme-1Pas (after 12 hours' incubation) increased in a linear manner from ~10 to ~180 mean fluorescent reading units at dosages of 0 to 12 μmol/L, respectively (data not shown).

The expression of ATF3 mRNA was evaluated by reverse transcription-PCR. The results demonstrated that ATF3 DNAzyme-1Pas oligonucleotide treatment resulted in the eradication of AFT3 mRNA expression by 1 day and after 3- and 5-day intervals (Fig. 4A, *lanes 2* to *4*), respectively). Following the addition of fresh media and the removal of the DNAzyme-1Pas, the cells recovered the expression of ATF3 mRNA after 2 to 4 days (Fig. 4A, *lanes 5* and *6*, respectively). Control experiments with the ATF3 DNAzyme-1Ps (sense) strand oligonucleotide failed to eradicate the ATF3 mRNA after 1 to 5 days' incubation (Fig. 4B, *lanes 1* to *4*). In addition, β-actin mRNA levels (and Sp1 mRNA levels; data not shown) were not affected by either oligonucleotide (Fig. 4A and B, *lower band*).

In experimental studies, reverse transcription-PCR was performed to examine ATF3 mRNA levels in CPTX-1532 cells (Fig. 4C). ATF3 mRNA levels normalized to that measured in untreated cells (*black*) were reduced by 10 μmol/L (~55 μg/mL) ATF3 DNAzyme-1Pas to barely detectable levels after 2, 3, and 5 days (*white*). The ATF3 DNAzyme-1Ps

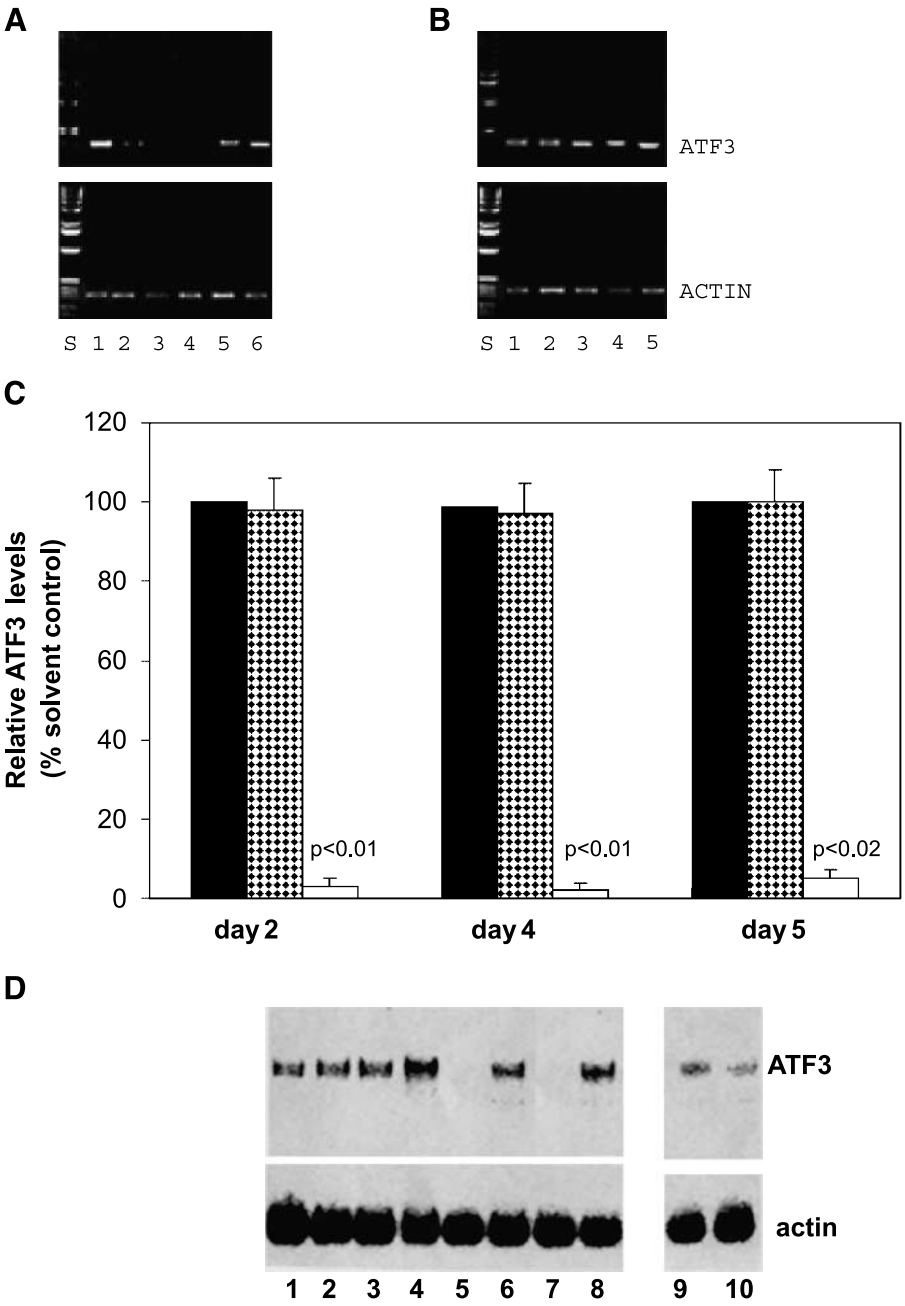


**FIGURE 4.** Reverse transcription-PCR (35 cycles) of ATF3 mRNA (363 bp): (**A**) ATF3 DNAzyme-1Pas and (**B**) ATF3 DNAzyme-1Ps. *Lower bands,* β-actin control (693 bp). Treatment was with 5 μmol/L ATF3 DNAzyme-1P for 2 hours (*lane 1*), 1 day (*lane 2*), 3 days (*lane 3*), and 5 days (*lane 4*). Recovery in fresh medium was for 2 days (*lane 5*) and 4 days (*lane 6*). *S,* molecular weight standards. Cells were plated at $1 \times 10^7$ per T25 flask and treated with a single dosage (5 μmol/L) of the ATF3 DNAzyme-1P on day 1. On day 5, cells were washed with fresh medium and incubated in fresh medium for 2 to 4 days. **C.** Reverse transcription-PCR (35 cycles) analysis of ATF3 mRNA expression after 2, 3, and 5 days of treatment of CPTX-1532 cells with 10 μmol/L ATF3 DNAzyme-1P. Cells were untreated (*black*) or treated with 10 μmol/L AFT3s (*checkerboard*) or ATF3as (*white*) oligonucleotide. ATF3 DNAzyme-1P (10 μmol/L) was ~55 μg/mL. **D.** Western blots with ATF3 antibodies (1:200 dilution) of crude protein extracts from CPTX-1532 cells treated with 5 μmol/L ATF3 DNAzyme-1Pas (*lanes 1*, *3*, *5*, *7*, and *9*) and ATF3 DNAzyme-1Ps (*lanes 2*, *4*, *6*, *8*, and *10*) oligonucleotides for 2 hours (*lanes 1* and *2*), 1 day (*lanes 3* and *4*), 2 days (*lanes 5* and *6*), 5 days (*lanes 7* and *8*), and 5 days (*lanes 9* and *10*). *Lower band,* β-actin.

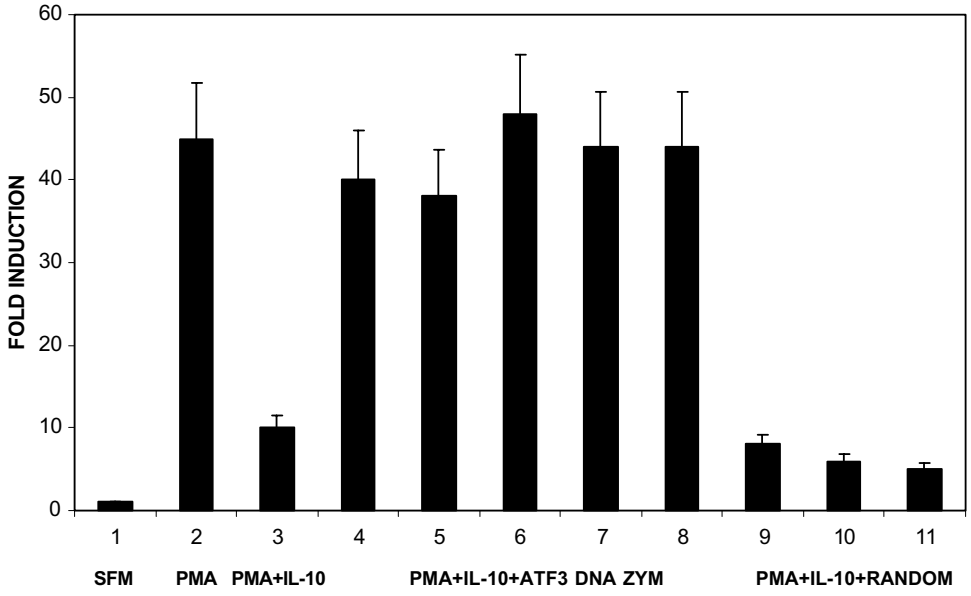


**FIGURE 5.** Luciferase assays with the MMP-2 luciferase reporter D7 construct (0.4 μg) in transiently transfected CPTX-1532 cells. Relative fold induction by SFM (*column 1*), PMA (*column 2*), PMA + IL-10 (*column 3*), and PMA (*columns 4* to *11*). Pretreatment of cells with 1, 2, 4, 10, and 20 μmol/L ATF3 DNAzyme-1Pas oligonucleotide (*columns 4* to *8*) and 4, 10, and 20 μmol/L ATF3 DNAzyme-1Ps oligonucleotide (*columns 9* to *11*). *Columns,* mean of three independent experiments; *bars,* SD. Compared with treatment with PMA, $P < 0.002$ (*columns 3* and *9* to *11*) and $P > 0.891$ (*columns 4* to *8*).

oligonucleotide (*checkerboard*) failed to reduce the ATF3 mRNA significantly after 2, 3, and 5 days. Taken together, the data indicated there was a sequence-specific inhibition of ATF3 mRNA by ATF3 DNAzyme-1Pas.

Western blots (21) of crude protein extracts from CPTX-1532 cells treated with ATF3 DNAzyme-1Pas oligonucleotides (5 μmol/L) showed that ATF3 protein levels dropped by ~50% after 1 day and that ATF3 was undetectable after 2 to 5 days treatment, respectively (Fig. 4D, *lanes 2*, *4*, *6*, and *8*). In comparison, treatment of the cells with ATF3 DNAzyme-1Ps oligonucleotides failed to "knock out" ATF3 expression, respectively (Fig. 4D, *lanes 1*, *3*, *5*, and *7*). Recovery studies helped validate the results. Following removal of the DNAzyme-1P oligonucleotides from the medium, ATF3 expression was restored after ~2 days' incubation (Fig. 4D, *lanes 9* and *10*). Finally, Western blots with β-actin antibodies showed that the expression of this protein was not influenced by either ATF3 DNAzyme-1P oligonucleotide. Densitometric scans (A600 nm; from three separate experiments) showed that the ratio of ATF3/β-actin was 0.22 ± 0.08, 0.23 ± 0.06, 0.21 ± 0.05, 0.25 ± 0.07, 0.22 ± 0.07, and 0.25 ± 0.08 for Fig. 4D, *lanes 1* to *4*, *6*, and *8*, respectively (with $P > 0.537$ compared with untreated cells). In comparison, the ratio of ATF3/β-actin was 0, 0, 0.11 ± 0.07, and 0.1 ± 0.08 for Fig. 4D, *lanes 5*, *7*, *9*, and *10*, respectively. The $P$ values were 0.001 and 0.189 for Fig. 4D, *lanes 5* and *7*, and Fig. 4D, *lanes 9* and *10*, respectively (compared with untreated cells).

### *MMP-2 Promoter Luciferase Assays Showing That IL-10 Blocks ATF3 Signaling/Induction of MMP-2 Expression*

On the basis of the above results, we hypothesized that "knockout" of ATF3 expression with the ATF3 DNAzyme-1Pas oligonucleotide should block IL-10–dependent suppression of D7 luciferase activity in vivo. For this purpose, CPTX-1532 cells were transiently transfected with the MMP-2 luciferase D7 promoter construct overnight and exposed overnight to ATF3 DNAzyme-1Pas oligonucleotide (i.e., at 1, 2, 4, 10, and 20 μg/mL; Fig. 5). As predicted, treatment of these cells with PMA + IL-10 (15 ng/mL) stimulated a significant increase in D7 luciferase activity (Fig. 5, *columns 4* to *8*). If these cells were transferred to fresh medium for 48 hours, IL-10 + PMA induced a 4- to 5-fold increase in the luciferase activity (data not shown). In control experiments, in cells treated overnight with ATF3 DNAzyme-1Ps oligonucleotide, IL-10 blocked PMA induced luciferase activity (Fig. 5, *columns 9* to *11*). Serum-free medium (SFM) failed to stimulate any luciferase activity in the latter experiments (Fig. 5, *column 1*). Other controls showed that PMA stimulated luciferase activity and IL-10 blocked PMA induced luciferase activity by ~4.5-fold (i.e., in the absence of the ATF3 DNAzyme-1Pas treatment), as predicted by previous experiments. In summary, these results demonstrate that the IL-10/IL-10R cascade specifically activates ATF3 signaling to block MMP-2 expression.

### *IL-10 Transfected CPTX-1532 Cells Express MMP-2 Following Treatment With ATF3 DNAzyme-1Pas*

To evaluate the effects of physiologic levels of IL-10 on ATF3 and MMP-2 expression, CPTX-1532 cells were stably transfected with the IL-10 gene. The transfected cells normally secreted nanogram amounts of IL-10 in the medium after 5 to 10 passages. Figure 6A demonstrated that the parent CPTX-1532 cells normally expressed IL-10 (*white*), ATF3 (*checkerboard*), MMP-2 (*crosshatched*), and MMP-9 (*diagonal stripes*). Following treatment with PMA, the levels of MMP-2 and MMP-9 expression were significantly elevated by ~2- to 3-fold compared with the untreated parent cells. However, PMA did not influence the levels of IL-10, ATF3, or β-actin in the parent cells and in the IL-10 mock or transfected CPTX-1532 subclones. More importantly, in the IL-10 transfected subclones, the levels of MMP-2 and MMP-9 dropped by ~10- and ~5-fold, respectively, and PMA failed to stimulate any increase in expression of either MMP-2 or MMP-9 protein in these cells (Fig. 6A). Data from three experiments indicated

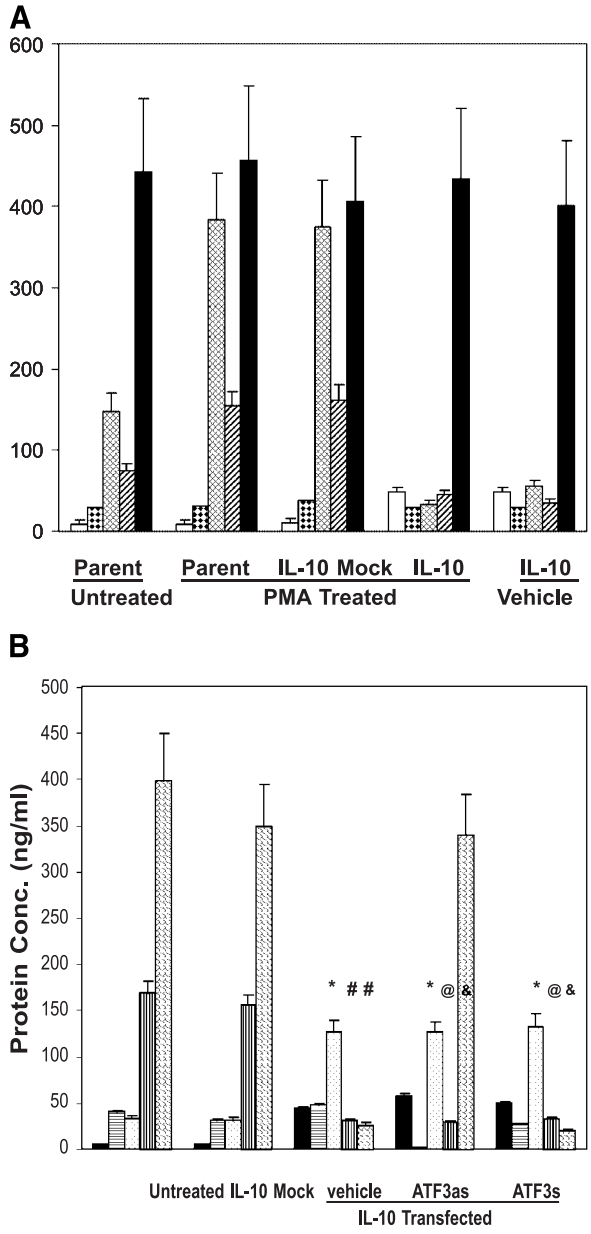


**FIGURE 6.** **A.** ELISA of IL-10 (*white*), ATF3 (*checkerboard*), MMP-2 (*crosshatched*), MMP-9 (*diagonal stripes*), and β-actin (*black*) levels expressed in the parent, IL-10 mock, and IL-10 transfected (*IL-10*) CPTX-1532 cells. Cells ($1 \times 10^7$) were either untreated or treated with PMA (100 μmol/L for 6 hours) or vehicle. Data from three experiments indicated that, in comparison with the parent cells, there was little difference in MMP-2 levels in PMA treated cells: parent (*, $P > 0.471$) and IL-10 mock (*, $P > 0.488$) cells. There was a significant reduction of MMP-2 (#, $P < 0.002$) and MMP-9 (#, $P < 0.003$) in PMA treated cells transfected with IL-10 and in vehicle treated cells transfected with IL-10. **B.** ELISA of IL-10 (*black*), ATF3 (*horizontal stripes*), TIMP-1 (*dotted*), MMP-9 (*vertical stripes*), and MMP-2 (*crosshatched*) levels. Cells were untreated parent, IL-10 mock transfected, and IL-10 transfected cells. The IL-10 transfected cells were exposed to vehicle, ATF3 DNAzyme-1Ps oligonucleotide (*ATF3s*), or ATF3 DNAzyme-1Pas oligonucleotide (*ATF3as*) at concentrations of 10 μmol/L for 12 hours. IL-10 induced a significant increase in TIMP-1 (*, $P < 0.001$) and reduced both MMP-9 and MMP-2 expression (#, $P < 0.001$ and #, $P < 0.002$). The ATF3 DNAzyme-1Pas oligonucleotide has no effect on TIMP-1 (*, $P > 0.399$) or MMP-9 (@, $P > 0.672$) but increased MMP-2 levels (@, $P < 0.002$) compared with vehicle. The ATF3 DNAzyme-1Ps oligonucleotide did not influence TIMP-1 (*, $P > 0.419$), MMP-9 (@, $P > 0.541$), and MMP-2 (&, $P > 0.721$).

that, in comparison with the parent cells, there was little difference in MMP-2 levels in PMA treated cells: parent (*, $P > 0.471$) and IL-10 mock (*, $P > 0.488$). There was a significant reduction of MMP-2 (#, $P < 0.002$) and MMP-9 (#, $P < 0.003$) in PMA treated cells transfected with IL-10 and in vehicle treated cells transfected with IL-10, respectively.

Figure 6B further showed that untreated and mock IL-10 transfected CPTX-1532 cells normally express little or no IL-10 (*black*) but do express ATF3 (*horizontal stripes*), TIMP-1 (*dotted*), MMP-9 (*vertical stripes*), and MMP-2 (*cross-hatched*). In stable IL-10 transfected cells, ATF3 levels are unchanged, but the IL-10 and TIMP-1 levels are significantly elevated and both MMP-9 and MMP-2 levels are significantly diminished to near background levels. Following treatment of these cells with the ATF3 DNAzyme-1Pas (*ATF3as*), ATF3 is undetectable (*horizontal stripes*) and MMP-2 levels (*cross-hatched*) are comparable with that found in IL-10 mock transfected cells. However, IL-10, TIMP-1, and MMP-9 levels are similar to that found in the IL-10 transfected cells treated with vehicle, indicating that AFT3 may selectively control MMP-2 expression. Control experiments with the ATF3 DNAzyme-1Ps (*ATF3s*) did not influence the levels of IL-10, ATF3, TIMP-1, MMP-9, or MMP-2 expression in comparison with the IL-10 transfected cells. Statistical analysis of data from three experiments indicated IL-10 induced a significant increase in TIMP-1 (*, $P < 0.001$) and reduced both MMP-9 and MMP-2 expression (#, $P < 0.001$ and #, $P < 0.002$). The ATF3 DNAzyme-1Pas oligonucleotide has no effect on TIMP-1 (*, $P > 0.399$) or MMP-9 (@, $P > 0.672$) but resulted in a significant increase in MMP-2 levels (@, $P < 0.002$) compared with vehicle. The ATF3 DNAzyme-1Ps oligonucleotide did not influence TIMP-1 (*, $P > 0.419$), MMP-9 (@, $P > 0.541$), and MMP-2 (&, $P > 0.721$), respectively.

Taken together, the data indicate that IL-10 requires the expression of ATF3 to specifically down-regulate MMP-2 expression.

## Discussion

Selective inhibition of MMP-2 or MMP-9 expression can abrogate human tumor cell invasion in in vitro and in vivo experiments (1, 13-18, 22). Likewise, ectopic expression of MMP-2 results in a metastatic phenotype in rat embryo cell lines, while inhibition of MMP-9 by ribozymes suppresses the metastatic capability of H-*ras*– and v-*myc*–transformed rat embryo cell lines (15, 16). Given the potentially crucial role of MMP-2 and MMP-9 in tumor invasion and angiogenesis, it is important to understand the molecular mechanisms by which MMP-2/MMP-9 expression might be inhibited in malignant cells.

Transcriptional regulation of MMP-2 is believed to be the most important component for MMP-2 expression (13, 17, 23). The human *MMP-2* gene has a 2.2-kb promoter region, but the proximal 670-bp promoter sequence contains all the essential transcription regulatory components (13). Important *cis*-acting elements include two AP-1 sites, nuclear factor-κB, Sp1, GT box, and PEA3 elements. It is generally accepted that maximal induction of MMP-2 gene expression requires all these *cis*-acting elements, although the proximal AP-1 site plays an indispensable role in MMP-2 gene transcription (22-24).

Unfortunately, the mechanisms of MMP-2 gene activation in human cancer cells are not well defined (23). Originally, the *MMP-2* gene has been thought to be refractory to modulation due to a lack of potential regulatory elements in the MMP-2 promoter (25). However, a recent study demonstrated that the human MMP-2 promoter contains several *cis*-acting regulatory elements and that several transcription factors including Sp1, Sp3, and AP-2 participate in the control of constitutive MMP-2 gene expression (24, 25). In addition, different signal transduction pathways can modulate expression of MMP-2. For example, activation of the Akt kinase signaling pathway may stimulate MMP-2 activity and tumor invasion (26), whereas activation of the phosphatase and tensin homologue, a dual specificity phosphatase that effectively attenuates Akt activity, may suppress MMP-2 expression and metastasis (22). Recent studies showed that nonsteroidal anti-inflammatory drugs (i.e., IL-10) exert potent antiangiogenesis and antimetastasis activity both in vitro and in vivo (27). Likewise, a previous study demonstrated that A549 human lung cancer cells expressed a high level of MMP-2 and that IL-10 and indomethacin inhibited MMP-2 expression and enzymatic activity in these cells (28). They also showed that IL-10 suppressed MMP-2 via inhibition of gene transcription (28). In this article, we address the molecular mechanism by which IL-10 inhibit MMP-2 expression.

There is a growing body of evidence that IL-10 can block the aberrant expression of MMP-2 and serve as a therapeutic agent for the prevention of tumor invasion, angiogenesis, and metastasis (13, 18). In this article, we investigated the effects of IL-10 on MMP-2 expression in a primary human prostate tumor line (CPTX-1532). Our results demonstrated that IL-10 significantly inhibited MMP-2 transcription and protein expression induced by a phorbol ester (PMA). IL-10 specifically induced tyrosine phosphorylation of ATF3, rapid nuclear translocation, and binding to the CREB consensus domain upstream of the 5′ transcriptional start site of the MMP-2 promoter. ATF3 binding to the CREB domain resulted in a significant down-regulation of promoter luciferase activity. EMSAs confirmed the data, and immunoblot assays of ATF3 immunoprecipitates with tyrosine specific antibodies further revealed that IL-10 stimulated tyrosine phosphorylation of ATF3 to activate binding to the CREB domain and suppress MMP-2 expression. Studies with stable IL-10 transfected CPTX-1532 subclones further showed that, in cells treated with a ATF3 DNAzyme-1Pas oligonucleotide, ATF3 expression was eliminated and IL-10 failed to suppress MMP-2 expression in these cells, albeit MMP-9 expression was down-regulated. Taken together, these data demonstrate the critical role of tyrosine phosphorylated ATF3 and the CREB consensus domain (29) in IL-10 suppression of MMP-2 gene expression in human prostate tumor cells.

Previous studies in our laboratory have shown that IL-10 and IL-4 down-regulated MMP-2 mRNA and protein levels in human prostate PC-3ML cells in vitro and in vivo in severe combined immunodeficiency mice tumors (18). In addition, we have shown that IL-10 blocked MMP-2 and MT1-MMP transcription and protein synthesis in HPCA-10 lines (13). Specifically, IL-10 suppressed insulin-like growth factor-I/insulin-like growth factor-I receptor axis induction of MMP-2 and MT1-MMP synthesis. Transient transfection experiments and chloramphenicol acetyltransferase assays with different regions of the 5′ promoter region of the *MMP-2* gene (−1,659 to −555 bp) showed that insulin-like growth factor-I stimulated p53-dependent pCAT activity and that IL-10 blocked insulin-like growth factor-I induced pCAT activity. EMSAs further indicated that IL-10 induced protein(s) binding to a putative "silencer elements termed S1 and S2" immediately downstream (−1,305 to −555 bp) of the p53 binding site (−1,649 to −1,630 bp). In this article, studies with the different MMP-2 promoter luciferase constructs confirmed these results and showed that IL-10 exerted a greater degree of suppression of the luciferase activity in cells transfected with the WT, D1, and D2 constructs containing the S1 and S2 elements (i.e., compared with the truncated D3-D7 fragments, which did not contain the S1 and S2 elements). In addition, we identified a CREB element downstream of the S1/S2 elements, which IL-10 controlled to block MMP-2 expression. At this juncture, we have now identified at least three suppressor elements, which are responsive to IL-10 signaling (i.e., S1, S2, and CREB) to block MMP-2 expression.

Note that in agreement with the earlier work on PC-3 ML and HPCA-10 cells, IL-10 also inhibited MMP-9 expression and stimulated TIMP-1 expression in the CPTX-1532 cells. The data therefore consistently suggest that the antitumor and antiangiogenic functions of IL-10 may reflect inhibitory effects on MMP-2 and MMP-9 expression combined with the up-regulation of TIMP-1 expression.

Unfortunately, ATF3 has only been partially characterized, and further work is required to understand its role in transcriptional regulation of MMP-2. ATF3 is a member of the mammalian ATF/CREB family of transcription factors (30-36). Members of the ATFI CREB family bound to a consensus DNA sequence (TGACGTCA) have a similar DNA binding domain, the basic region leucine zipper domain, and form selective heterodimers with each other through the leucine zipper region. The ATF1CRE or ATF1CRE-like sites are present in many promoters and mediate transcriptional responses to a variety of signals such as cAMP (34), adenovirus E1A (35-37), viral induction (38), cytokine induction (39-41), and DNA damage (42). Unfortunately, it is not clear how ATFI CREB proteins control the expression of these potential target promoters. Apparently, different ATFI CREB proteins mediate different transcriptional responses. Of relevance to the data reported in this article, a recent article (29) has shown that, contrary to the implication of its name, ATF represses rather than activates transcription from promoters with ATF sites. Apparently, it represses transcription by stabilizing inhibitory cofactors at the promoter. Our data agree with these results and provide strong evidence that the IL-10/IL-10R axis signaling of ATF3 and CREB represses MMP-2 promoter activity.

DNAzymes are single-stranded oligodeoxynucleotide with enzymatic activity. The "10-23" catalytic DNAzyme motif (43) employed in this article can cleave effectively any unpaired purine and pyrimidine of mRNA transcripts (43). For example, a DNAzyme targeting vascular endothelial growth factor receptor 2 has been developed to inhibit tumor angiogenesis (44). Marked cell death in the peripheral regions of the tumor accompanied by a reduction in blood vessel density was observed

after DNAzyme administration in breast tumor–bearing mice. Similarly, DNAzymes designed to target expression of $\beta_1$ and $\beta_3$ integrin mRNA specifically decreased the cell surface expression of corresponding subunits in endothelial cells and K562 cells (43). In functional tests, $\beta_{1\text{-}1,053}$ and $\beta_{3\text{-}1,243}$ markedly reduced adhesion of cells to fibronectin and vitronectin, respectively. In our studies, we designed a DNAzyme (31 bp), which consisted of a 15-deoxynucleotide catalytic domain ("10-23" motif) that was flanked by two substrate recognition segments of eight deoxynucleotides for the 5′ start codon of the ATF3 mRNA, respectively. The ATF3 DNAzyme-1Pas construct was shown to specifically cleaved its substrate, whereas the ATF3 DNAzyme-1Ps construct did not cleave ATF3 mRNA. The ATF3 DNAzyme-1Pas treatment abolished ATF3 protein expression and blocked IL-10 inhibition of MMP-2 expression. In conclusion, we found that ATF3 DNAzyme-1Pas was potentially useful as a gene-inactivating agent and may ultimately provide a therapeutic means to inhibit tumor growth and angiogenesis in vivo.

## Materials and Methods

### *Cell Cultures*

CPTX-1532 cells (kindly provided by Drs. Robert Bright and Susan Topalian, National Cancer Institute, NIH, Bethesda, MD) were derived from normal human prostate tissue and immortalized with human papillomavirus serotype 16 (19). The cells were maintained in keratinocyte SFM (Life Technologies, Inc., Grand Island, NY) containing 5 ng/mL epidermal growth factor, 50 μg/mL bovine pituitary extract, and 5% fetal bovine serum (Biofluids, Rockville, MD) + 100 units/mL penicillin G sodium and 100 μg/mL streptomycin sulfate. Cells were cultured at 37°C in a humidified atmosphere of 95% air and 5% $CO_2$. In experimental studies, the cells were harvested using 0.08 mol/L sodium citrate (pH 8.0), washed three times with fresh keratinocyte SFM, counted with a hemacytometer, and plated (in keratinocyte SFM + dihydrotestosterone containing 10 mmol/L HEPES) 4 hours prior to starting experimental treatments.

### *MMP-2 Promoter Studies*

The MMP-2 promoter was a gift of Bian and Sun (Parke Davis Inc., Chicago, IL; ref. 20). A 1,746-bp DNA fragment (−1,659 to +57 bp) upstream from the transcription initiation site of the *MMP-2* gene was PCR amplified with Expand High Fidelity DNA polymerase (Boehringer-Mannheim, Chicago, IL). The primers used were T4.01 (5′-CACACCCACCAGACAAGCCT-3′) and T4.02 (5′-AAGCCCCAGATGCGCAGCCT-3′). Both strands were sequenced with the DNA Sequenase Kit (Amersham, Chicago, IL) as well as with an automatic DNA sequencer (ABI Prism 377 DNA sequencer). There was 100% homology with the published sequence for human MMP-2 promoter (45). Price et al. (46) and Koul et al. (22) have functionally characterized an entire panel of *cis*-acting promoter elements, extending over a 2-kb interval of the MMP-2 promoter.

The human *MMP-2* gene has a ~2.2-kb promoter region, but the proximal 670-bp promoter sequence contains all the essential transcription regulatory components. Important *cis*-acting elements include two AP-1 sites, nuclear factor-κB, Sp1, GT box, and PEA3 elements. It is generally accepted that maximal induction of MMP-2 gene expression requires all these *cis*-acting elements, although the proximal AP-1 site plays an indispensable role in MMP-2 gene transcription (24).

EMSA was performed using the following oligonucleotides as probes and/or competitors: the oligonucleotide Sp1A has the sequence 5′-CAGAGAGGGGCGGGCCCGAGTG-3′ and corresponds to the human MMP-2 promoter sequence 98 to 76 and the AP-2 oligonucleotide has the sequence 5′-CCCCAGCCCCGCTCTGCCAGCT-3′ and corresponds to the human MMP-2 promoter sequence 66 to 44. The mutant Sp1 oligonucleotide has the sequence 5′-CAGATATCTAGATGATATCGTG-3′ and the mutant AP-2 oligonucleotide is 5′-CCGATATCATCTAGAATCAGCT-3′.

A luciferase reporter plasmid driven by 1,659 bp of the human MMP-2 promoter was used in this study and is called WT (13, 47). Pfu DNA polymerase synthesized serial deletion mutants using PCR according to methods of Qin et al. (24). This permitted the synthesis of MMP-2 promoter fragments with specific deletions of *cis*-acting regulatory elements in the MMP-2 promoter (Fig. 7). Specific primers for each MMP-2 promoter fragment included (D1) 5′-CTCTGGGTTCGGCGTCTCTGAAAAGATCGA-3′, (D2) 5′-ACAAGGGACGACTGGGGGTCAGGATAGACGGGGG-3′, (D3) 5′-GAGAAGTCCAGAGTCGAGTCTTCAGTGAAGAA-3′, (D4) 5′-GAAGGTCCTTCGGAAGGAACTAACAGAAATGATCAA-3′, (D5) 5′-CCGCGTCCTTTCCTAAGTTCTCACTCACCCCTTAAA-3′, (D6) 5′-AACGTCTTCCTTTCTCCATTCCTTCGTTGGACCC-3′, (D7) 5′-TCCTTCGTTGGGCCCTGGAAGGTGACAAAGACAA-3′, (D8) 5′-TCTTTCCTTTTTTCACCTCTTTTCACCTCTCTCCCC-3′, (D9) 5′-GATCTCGCTGTCTACAAAGGGTCGTCCCCCAAGGCTCC-3′, (D10) 5′-TTTCACCTCCTCCCGCTCATCCCCCCGCCCCGTC-3′, (D11) 5′-CACGCGGGGGGCGGGGGTCGGGGCGGGACGT-3′, and (D12) 5′-ACCGCCGGCGGGGGGGAACAAAGGCGGCGTAGGTCT-3′.

### *Plasmids, Transient Transfection, and MMP-2 Promoter Luciferase/β-Galactosidase Assays*

A luciferase reporter plasmid driven by the human MMP-2 promoter was used in this study (24, 47), and the reporter vector pTKβ (Clontech, Palo Alto, CA) expressing β-galactosidase under control of the herpes simplex virus thymidine promoter was used as an internal reference plasmid. The hCIITAp1.7 construct, in which the luciferase gene is under control of the type IV promoter of the human class II transactivator (*CIITA*) gene, was described previously (24). In brief, MMP-2 promoter constructs (10 μg) were cotransfected into human CPTX-1532 cells with 1 μg pTKβ-galactosidase construct into $3 \times 10^6$ cells by electroporation with a Gene Pulser (Bio-Rad, Hercules, CA) set at 250 V, 960 μF, as described previously (48). After transfection, cells were allowed to recover for 24 hours and cultured in 1% fetal bovine serum/keratinocyte SFM for 48 hours. Cells were washed with PBS and lysed with 200 μL of lysis buffer containing 25 mmol/L trisphosphate (pH 7.8), 2 mmol/L DTT, 2 mmol/L diaminocyclohexane tetraacetic acid,

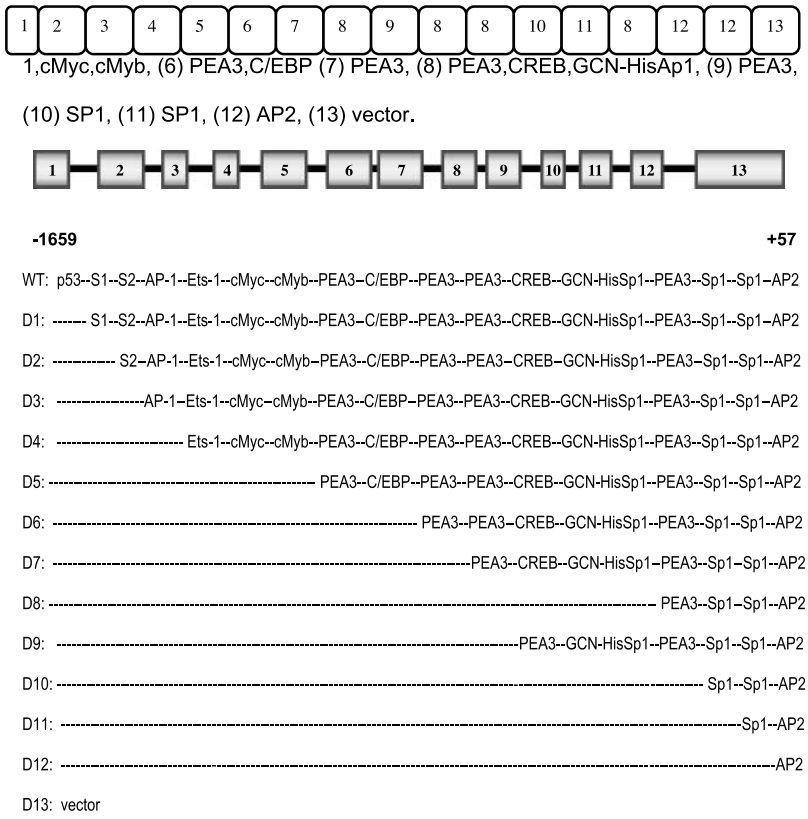


**FIGURE 7.** Synthesis of MMP-2 promoter fragments with specific deletions of *cis*-acting regulatory elements in the MMP-2 promoter. D1, which lacks the p53 site; D2, which lacks the first silencer element (S1); D3, which lacks both silencer elements (S1 and S2); D4, which lacks the AP-1 element; D5, which lacks the Ets-1 and c-Myc/c-Myb sites; D6, which lacks one PEA3 site and the CAAT/enhancer binding protein element; D7, which lacks the second PEA3 site; D8, which lacks the third PEA3 site, the CREB site, and GCN-His region; D9, which lacks the CREB site; D10, which lacks the fourth PEA3 site; D11, which lacks the first Sp1 element; D12, which lacks both Sp1 elements; and D13, which lacks the AP-2 site.

10% glycerol, and 1% Triton X-100. Extracts were assayed in triplicate for luciferase activity in a volume of 250 μL containing 50 μL cell extract, 25 mmol/L Tris, 0.1 mmol/L EDTA, 1 mmol/L $MgCO_3$, 2.67 mmol/L $MgSO_4$, 33.3 mmol/L DTT, 0.27 mmol/L CoA, 0.47 mmol/L luciferin, and 0.55 mmol/L ATP, and light intensity was measured using a Luminometer (Promega, Madison, WI). Luciferase activity was integrated over a 10-second time period. Extracts were also assayed in triplicate for β-galactosidase enzyme activity as described previously (45, 48, 49). The luciferase activity of each sample was normalized to β-galactosidase activity to calculate relative luciferase activity before calculating the fold activation value. The luciferase activity from the vector control was arbitrarily set at 1 for calculation of fold activation.

### *Reverse Transcription-PCR Studies of ATF3 Expression*

The PCR amplification protocol was according to Sambrook et al. (20). In brief, the protocol consisted of an initial 1-minute melting step at 94°C followed by 35 cycles with 50-second melting step at 92°C, 50-second annealing at 60°C, and 90-second extension at 75°C, except for the last cycle that contained a 5-minute extension step. The restriction enzyme *Eco*RI was used to check positive clones and *Ava*I was used to verify the correct orientation. The deletion mutants were inserted into the pGL2-Basic vector, which contains the gene for luciferase as reporter, using the *Kpn*I/*Xho*I restriction site.

### *IL-10 Transfection Studies*

Transient transfections were carried out according to previously published methods (18) using an Ad5CMV vector and the LipofectAMINE method (BRL, Bethesda, MD) according to methods described previously (20, 50). Cells were transfected with the Ad5CMV IL-10 sense cDNA constructs (51-53) overnight prior to experimental treatment of the cells. Controls included cells transfected with the Ad5CMV-LacZ control virus (i.e., mock transfections). Recombinant protein expression in the transfected cells was normalized for β-galactosidase.

### *ATF3 DNAzyme-1P Studies in IL-10 Transfected Cells*

The ATF3 DNAzyme-1Pas (31 bp) consisted of a 15-deoxynucleotide catalytic domain (“10-23” catalytic motif; ref. 43) that was flanked by two substrate recognition segments of eight deoxynucleotides for the 5′ start codon of the ATF3 mRNA, respectively (see bold base pairs below). ATF3

DNAzyme-1Ps strand sequences were used as a control. The DNAzymes were dissolved in keratinocyte SFM and stored at −20°C until use. DNAzymes were mixed with Lipofectamine (1:1 volume) for 1 hour prior to use, and cells were incubated with the mixture.

ATF3 DNAzyme-1Pas (antisense strand): 5′-**GACATGAA**-CAGGCTAGCTACAACGA**CACGCCTC**-3′ and ATF3 DNAzyme-1Ps (sense strand): 5′-**CTGTACTTG**CAGGCTAGCTACAACGA**TGCGGAG**-3′.

### *Flow Cytometric Analysis of ATF3 DNAzyme-1P Uptake in CPTX-1532 Cells*

For the time course studies, $1 \times 10^6$ cells per milliliter were incubated with 5 μmol/L FAM-labeled ATF3 DNAzyme-1Pas or unlabeled ATF3 DNAzyme-1Pas for various intervals according to the manufacturer of the FAM probe (Amersham, Arlington Heights, IL). For dose response studies, cells were incubated with 0, 0.1, 0.5, 1, 5 and 10 μmol/L FAM-labeled or unlabeled ATF3 DNAzyme-1Pas for 24 hours. Cells were harvested, washed three times with PBS at 4°C, and incubated with 0.2 mol/L acetic acid and 0.5 mol/L NaCl (pH 3) at 4°C for 10 minutes. Cells were washed twice with fresh PBS and incubated with 6 μg/mL propidium iodide (Calbiochem, La Jolla, CA) for 30 minutes. Green fluorescence of propidium iodide negative cells was measured by flow cytometry. The relative amount of intracellular ATF3 DNAzyme-1Pas was expressed as the ratio of the mean fluorescence intensities of FAM-labeled ATF3 DNAzyme-1Pas and unlabeled ATF3 DNAzyme-1Pas treated cells.

### *EMSA of ATF3 Expression in Untreated and Treated CPTX-1532 Cells*

Nuclear and cytoplasmic protein extracts were prepared as described previously (50) and as adopted from Finbloom and Winestock (51). Cells were grown in 100 mm dishes, allowed to adhere overnight, and incubated in SFM for 24 hours. Cells were washed with cold PBS, harvested by scraping, and pelleted. Cells were resuspended in 1 mL of buffer A (10 mmol/L KCl, 20 mmol/L HEPES, 1 mmol/L $MgCl_2$, 1 mmol/L DTT, 0.4 mmol/L phenylmethylsulfonyl fluoride, 1 mmol/L NaF, and 1 mmol/L $Na_3VO_4$), incubated on ice for 10 minutes, and pelleted at 1,000 × *g* for 10 minutes. Pellets were resuspended in 0.5 mL of buffer A + 0.1% NP40, incubated on ice for 10 minutes, and centrifuged at 3,000 × *g* for 10 minutes. The nuclear pellet was resuspended in 1 mL of buffer B (10 mmol/L HEPES, 400 mmol/L NaCl, 0.1 mmol/L EDTA, 1 mmol/L $MgCl_2$, 1 mmol/L DTT, 0.4 mmol/L phenylmethylsulfonyl fluoride, 15% glycerol, 1 mmol/L NaF, and 1 mmol/L $Na_3VO_4$) and incubated for 30 minutes at 4°C with constant gentle mixing. Nuclei were pelleted at 40,000 × *g* for 30 minutes, and both cytoplasmic and corresponding nuclear extracts were dialyzed for 2 hours at 4°C against 1 L of buffer C (20 mmol/L HEPES, 200 mmol/L KCl, 1 mmol/L $MgCl_2$, 0.1 mmol/L EDTA, 1 mmol/L DTT, 0.4 mmol/L phenylmethylsulfonyl fluoride, 15% glycerol, 1 mmol/L NaF, and 1 mmol/L $Na_3VO_4$). Extracts were cleared by centrifugation at 14,000 × *g* for 15 minutes at 4°C.

For the EMSAs (28), 1 ng $^{32}$P-labeled oligonucleotide (20,000 cpm) 5′-AGAGATTGCC*TGACGTCA*GAGAGCTAG-3′ (CREB) was incubated for 30 minutes at room temperature with 10 μg crude nuclear protein extract in a volume of 20 μL containing 50 mmol/L KCl, 2.5 mmol/L $MgCl_2$, 1 mmol/L EDTA, 1 mmol/L DTT, 10 mmol/L Tris-HCl (pH 7.5), 10% glycerol, 1 μg salmon sperm DNA, and 1 μg poly(deoxyinosinic-deoxycytidylic acid). For antibody "supershift" analysis, 1 μL of antibody was incubated with the nuclear extracts at 4°C for 30 minutes in binding buffer followed by an additional incubation for 30 minutes at room temperature with labeled oligonucleotide. For cold competitions (51), unlabeled DNA was incubated with the nuclear extracts at 4°C for 20 minutes before addition of labeled probe. Bound and free DNAs were resolved by electrophoresis through a 6% polyacrylamide gel at 250 V in 0.25× Tris-borate EDTA (50 mmol/L Tris-HCl and 2 mmol/L EDTA). Dried gels were exposed to Kodak XAR-5 film at −70°C with intensifying screens. For cold competition assays, extracts were incubated with an excess of unlabeled CREB oligonucleotide. For supershift analysis (51), anti-ATF3 antibodies (Santa Cruz Biotechnology, Santa Cruz, CA) were added to the extracts 15 minutes before addition of the probe. Expression levels were measured in response to PMA, IL-10, or PMA + IL-10.

### *ELISA of IL-10, ATF3, TIMP-1, MMP-9, and MMP-2 Expression*

ELISAs were performed using standard curves developed for each antibody for converting the ELISA reading (A 600 nm) to amounts of protein (18, 53). In experiments, increasing amounts of crude protein extract (5, 10, 15, and 20 μg/mL) were applied to 96-well plates and air dried (three wells per protein concentration tested). Wells were blotted with an excess of each of the primary antibodies and avidin-biotin labeled peroxidase antiperoxidase secondary antibody (Sigma Chemical Co., St. Louis, MO). ELISA readings for the four different protein concentrations were averaged from triplicate wells per experiment, and the data were normalized for 10 μg crude protein extract. The amounts of each antigen (1 ng/10 μg total protein) in crude protein extract were calculated (mean ± 1 SD) from the standard curves developed for each antibody for converting ELISA readings to amounts of protein (18). Protein measurements were according to Bradford (54).

### *Western Blots of ATF3 Expression*

Western blots were according to methods of Towbin et al. (21) using well-characterized antibodies + peroxidase-antiperoxidase secondary antibodies (Sigma Chemical). Whole cell lysates were prepared by solubilization of the cells in buffer containing 0.1 mol/L Tris-HCl (pH 6.8), 0.1% SDS, 5% glycerol, 0.005% bromophenol blue, 0.005% pyronine Y, and 1% β-mercaptoethanol. Thirty microliters of buffer containing a lysate of $5 \times 10^4$ cells (10 μg protein per lane) were loaded per lane of SDS-PAGE gel with 10% running gel and 4.6% stacking gel. β-actin antibodies (Sigma Chemical) were used for control blots.

### *Immunoprecipitation Assays Measuring IL-10 Induction of ATF3 Phosphorylation/Signaling*

For immunoprecipitation, cell lysates of treated cells were prepared as described previously (50, 51). Total protein (500 μg)

was incubated with 4 μg polyclonal antisera to human ATF3 overnight. Protein A/G agarose beads were added for 2 hours at 4°C, and the immunoprecipitates were washed five times with lysis buffer, eluted from the agarose beads by boiling in 2× SDS sample buffer, and subjected to 8% SDS-PAGE. Proteins were transferred to nitrocellulose, and the membrane was blocked in 1% bovine serum albumin in TBS with 0.01% Tween 20 for 1 hour. The blots were incubated with anti-ATF3 monoclonal antibody (1 μg/mL) in an "antibody dilution buffer" (0.5% Tween 20, 1% bovine serum albumin, 10% glycerol, and 1 mol/L glucose in TBS) at 4°C overnight. The blots were washed and developed as described above. For reblotting, membranes were stripped at 56°C in buffer containing 100 mmol/L 2-ME, 2% SDS, and 62.5 mmol/L Tris-HCl (pH 6.7) with occasional shaking and reprobed with relevant antibodies.

### *Statistical Analysis*

Data analysis was performed using the SPSS statistical software package (SPSS, Chicago, IL). A two-sided Student's *t* test or a Welch's *t* test in unequal variances was used to determine differences between groups. Differences were considered statistically significant when $P < 0.05$. Data were plotted as means ± SD.

### *Source of Agents*

Human recombinant IL-10 was a generous gift from Narula Sawant (Schering-Plough Inc., Kennilworth, NJ). IL-10 and IL-10R antibodies were kindly provided by Schering-Plough and DNAX Research Institute of Molecular and Cellular Biology (San Diego, CA). The IL-10 cDNA was a generous gift of Kevin Moore (DNAX Research Institute of Molecular and Cellular Biology).

Stock solutions were made up in 0.9% NaCl solution (pH 7.2) and diluted in keratinocyte SFM prior to the treatment of cells. LipofectAMINE and FAM were purchased from Amersham, fetal calf serum was purchased from Biofluids, and keratinocyte SFM was purchased from Mediatech (Herndon, VA). β-galactosidase assay kit was purchased from Stratagene (La Jolla, CA), and IgG antibodies were purchased from Sigma Chemical. PMA and IFNγ were purchased from Sigma Chemical. Mouse anti-human MMP-2, MMP-9, and TIMP-1 monoclonal antibodies were bought from Sigma Chemical. Rabbit anti-human ATF3 polyclonal antibody and anti-ATF3 phosphotyrosine polyclonal antibody were purchased from Upstate Biotechnology (Lake Placid, NY). The secondary peroxidase-conjugated rabbit anti-human IgG antibodies and enhanced chemiluminescence reagents were from Amersham.

## References


1. Stetler-Stevenson WG, Hewitt R, Corcoran M. Matrix metalloproteinases and tumor invasion: from correlation and causality to the clinic. Semin Cancer Biol 1996;7:147-55.

2. Vu TH, Werb Z. Matrix metalloproteinases: effectors of development and normal physiology. Genes Dev 2000;14:2123-9.

3. Massova IL, Kotra P, Fridman R, Mobashery S. Matrix metalloproteinases: structures, evolution, and diversification. FASEB J 1998;12:1075-87.

4. Curran S, Murray GI. Matrix metalloproteinases in tumor invasion and metastasis. J Pathol 1999;189:300-9.

5. McCawley LJ, Matrisian LM. Matrix metalloproteinases: multifunctional contributors to tumor progression. Mol Med Today 2000;6:149-56.

6. Schonbeck U, Mach F, Libby P. Generation of biologically active IL-1β by matrix metalloproteinases: a novel caspase-1-independent pathway of IL-1β processing. J Immunol 1998;161:3340-8.

7. Manes S, Llorente M, Lacalle RA, et al. The matrix metalloproteinase-9 regulates the insulin-like growth factor-triggered autocrine response in DU-145 carcinoma cells. J Biol Chem 1999;274:6935-44.

8. Haro H, Crawford HC, Fingleton B, Shinomiya K, Spengler DM, Matrisian LM. Matrix metalloproteinase-7-dependent release of tumor necrosis factor-α in a model of herniated disc resorption. J Clin Invest 2000;105:143-51.

9. Powell WC, Fingleton B, Wilson CL, Boothby M, Matrisian LM. The metalloproteinase matrilysin proteolytically generates active soluble Fas ligand and potentiates epithelial cell apoptosis. Curr Biol 1999;9:1441-51.

10. Rao JS, Yamamoto M, Mohaman S, et al. Expression and localization of 92 kDa type IV collagenase/gelatinase B (MMP-9) in human gliomas. Clin Exp Metastasis 1996;14:12-22.

11. Liotta LA, Tryggvason K, Garbisa S, Hart I, Foltz CM, Shafie S. Metastatic potential correlates with enzymatic degradation of basement membrane collagen. Nature 1980;284:67-78.

12. Wood M, Fudge K, Mohler J, Frost A, Garcia F, Stearns ME. In situ hybridization studies of metalloproteinases 2 and 9 and TIMP-1 and TIMP-2 expression in human prostate cancer. Clin Exp Metastasis 1997;15: 246-58.

13. Stearns ME, Wang M, Hu Y, Garcia FU, Rhim J. IL-10 blocks MMP-2 and MT1-MMP synthesis in primary human prostate tumor lines. Clin Cancer Res 2003;9:1191-9.

14. Kondraganti S, Mohanam S, Chintala SK, et al. Selective suppression of matrix metalloproteinase-9 in human glioblastoma cells by antisense gene transfer impairs glioblastoma cell invasion. Cancer Res 2000;60:6851-9.

15. Hua J, Muschel RJ. Inhibition of matrix metalloproteinase 9 expression by a ribozyme blocks metastasis in a rat sarcoma model system. Cancer Res 1996; 56:5279-86.

16. Bernhard EJ, Gruber SB, Muschel RJ. Direct evidence linking expression of matrix metalloproteinase 9 (92-kDa gelatinase/collagenase) to the metastatic phenotype in transformed rat embryo cells. Proc Natl Acad Sci USA 1994; 91:4293-8.

17. Lacraz S, Nicod LP, Chicheportiche R, Welgus HG, Dayer J-M. IL-10 inhibits metalloproteinase and stimulates TIMP-1 production in human mononuclear phagocytes. J Clin Invest 1995;96:2304-10.

18. Stearns ME, Rhim J, Wang M. IL-10 inhibition of primary human prostate cell induced angiogenesis. IL-10 stimulation of TIMP-1 and inhibition of MMP-2/ MMP-9 secretion. Clin Cancer Res 1999;5:189-96.

19. Bright RK, Vocke CD, Emmert-Buck MR, et al. Generation and genetic characterization of immortal human prostate epithelial cell strains derived from primary cancer specimens. Cancer Res 1997;57:995-1002.

20. Sambrook J, Fritsh ED, Maniatis T. Molecular cloning. A laboratory manual. 2nd ed. Vol. 1. Plainview (NY): Cold Spring Harbor Laboratory Press. p. 2.82-2. 108;1989.

21. Towbin H, Staehelin T, Gordon J. Electrophoretic transfer of proteins from polyacrylamide gels to nitrocellulose sheets; procedures and some applications. Proc Natl Acad Sci USA 1979;76:4350-4.

22. Koul D, Parthasarathy R, Shen R, et al. Suppression of matrix metalloproteinase-2 gene expression and invasion in human glioma cells by MMAC/ PTEN. Oncogene 2001;20:6669-78.

23. Mauviel A. Cytokine regulation of metalloproteinase gene expression. J Cell Biochem 1993;53:288-95.

24. Qin H, Sun Y, Benveniste EN. The transcription factors Sp1, Sp3, and AP-2 are required for constitutive matrix metalloproteinase-2 gene expression in astroglioma cells. J Biol Chem 1999;274:29130-8.

25. Pan M-R, Hung W-C. Nonsteroidal anti-inflammatory drugs inhibit matrix metalloproteinase-2 via suppression of the ERK/Sp1-mediated transcription. J Biol Chem 2002;277:2775-80.

26. Park BK, Zeng X, Glazer RI. Akt1 induces extracellular matrix invasion and matrix metalloproteinase-2 activity in mouse mammary epithelial cells. Cancer Res 2001;61:7647-53.

27. Masferrer JL, Leahy KM, Koki AT, et al. Antiangiogenic and antitumor activities of cyclooxygenase-2 inhibitors. Cancer Res 2000;60:1306-11.

28. Pan MR, Chuang LY, Hung WC. Non-steroidal anti-inflammatory drugs inhibit matrix metalloproteinase-2 expression via repression of transcription in lung cancer cells. FEBS Lett 2001;508:365-8.

29. Hai T, Liu F, Coukos WJ, Green MR. Transcription factor ATF cDNA

clones: an extensive family of leucine zipper proteins able to selectively form DNA-binding heterodimers. Genes Dev 1989;3:2083-90.

30. Hoefler JP, Meyer TE, Yun Y, Jameson JL, Habener JF. Cyclic AMP-responsive DNA-binding protein: structure based on a cloned placental cDNA. Science 1988;242:1430-3.

31. Gonzalez GA, Yamamoto KK, Fischer WH, et al. A cluster of phosphorylation sites on the cAMP regulated nuclear factor CREB predicted by its sequence. Nature 1989;337:749-52.

32. Foulkes NS, Borrelli E, Sassone-Corsi P. CREM gene: use of alternative DNA binding domains generates multiple antagonists of cAMP-induced transcription. Cell 1991;64:739-49.

33. Lee CQ, Yun Y, Hoeffler JP, Habener JF. Cyclic AMP responsive transcriptional activation involves interdependent phosphorylated subdomains. EMBO J 1990;9:4455-65.

34. Foulkes NS, Sehlotter F, Pévet P, Sassone-Corsi P. Pituitary hormone FSH directs the CREM functional switch during spermatogenesis. Nature 1993; 362:264-7.

35. Lee KAW, Green MR. A cellular transcription factor E4F1 interacts with an E1A-inducible enhancer and mediates constitutive enhancer function in vitro. EMBO J 1987;6:1345-53.

36. Lee KA, Hai TY, SivaRaman L, et al. A cellular protein, activating transcription factor, activates transcription of multiple E1A-inducible adenovirus early promoters. Proc Natl Acad Sci USA 1987;84:8355-9.

37. Pei R, Berk AJ. Multiple transcription factor binding sites mediate adenovirus E1A transactivation. J Virol 1989;63:3499-506.

38. Garcia J, Wu F, Gaynor RT. Upstream regulatory regions required to sequence in an adenovirus early promoter RL. Nucleic Acids Res 1987;15: 8367-85.

39. Du W, Maniatis T. An ATF/CREB binding site is required for virus induction of the human interferon β gene. Proc Natl Acad Sci USA 1992;89:2150-4.

40. Hooft Van Huijsduijnen R, Whelan J, Pescini R, Becker-Andre AM, Deraemy-Schenk M, DeLamarter JF. A T-cell enhancer cooperates with NF-κB to yield cytokine induction of E-selectin gene transcription in endothelial cells. J Biol Chem 1992;267:22385-91.

41. Kaszubska W, Hooft van Huijsduijnen R, Ghersa P, et al. Cyclic AMP-independent ATF family members interact with NF-κB and function in the activation of the E-selectin promoter in response to cytokines. Mol Cell Biol 1993;13:7180-8.

42. Kedar PS, Widen SG, Englander EW, Fornace AJJ, Wilson SH. The ATF/CREB transcription factor-binding site in the polymerase β promoter mediates the positive effect of *N*-methyl-*N'*-nitro-*N*-nitrosoguanidine on transcription. Proc Natl Acad Sci USA 1991;88:3729-33.

43. Cieslak M, Niewiarowska J, Nawrot M, Koziolkiewicz, M, Stec WJ, Cierniewski CS. DNAzymes to β1 and β3 mRNA Down-regulate expression of the targeted integrins and inhibit endothelial cell capillary tube formation in fibrin and Matrigel. J Biol Chem 2002;277:6779-87.

44. Zhang L, Gasper WJ, Stass SA, Loffe OB, Davis MA, Mixson AJ. Angiogenic inhibition mediated by a DNAzyme that targets vascular endothelial growth factor receptor 2. Cancer Res 2002;62:5463-9.

45. Bian J, Sun Y. Transcriptional activation by p53 of the human type IV collagenase (gelatinase A or matrix metalloproteinase 2) promoter. Mol Cell Biol 1997;17:6330-8.

46. Price SJ, Greaves DR, Watkins H. Identification of novel, functional genetic variants in the human matrix metalloproteinase-2 gene. J Biol Chem 2001; 278:7549-58.

47. Qin H, Moellinger JD, Wells A, Windsor LJ, Sun Y, Benveniste EN. Transcriptional suppression of matrix metalloproteinase-2 gene expression in human astroglioma cells by TNFα- and IFN-γ. J Immunol 1998;161:6664-74.

48. Dong Y, Rohn WM, Benveniste EN. IFN-γ regulation of the type IV class II transactivator promoter in astrocytes. J Immunol 1999;162:4731-9.

49. Sehgal I, Thompson TC. Novel regulation of type IV collagenase (matrix metalloproteinase-9 and -2) activities by transforming growth factor-β1 in human prostate cancer cell lines. Mol Biol Cell 1999;10:407-13.

50. Wang M, Hu Y, Shima I, Stearns ME. Identification of positive and negative regulator elements for the tissue inhibitor of metalloproteinase 1 gene. Oncol Res 1998;10:219-33.

51. Finbloom DS, Winestock KD. IL-10 induces the tyrosine phosphorylation of tyk2 and Jak1 and the differential assembly of STAT1α and STAT3 complexes in human T cells and monocytes. J Immunol 1995;155:1079-90.

52. Stearns ME, Wang M. Antimetastatic and antitumor activities of interleukin 10 in transfected human prostate PC-3 ML clones. Orthotopic growth in SCID mice. Clin Cancer Res 1998;4:2257-63.

53. Stearns ME, Garcia FU, Fudge KA, Wang M. Role of IL-10 and TGF-1 in the angiogenesis and metastasis of prostate primary tumor lines from orthotopic implants in SCID mice. Cancer Res 1999;5:711-20.

54. Bradford MM. A rapid and sensitive method for the quantitation of microgram quantities of protein utilizing the principles of protein-dye binding. Anal Biochem 1976;72:248-54.